

# The origin of pelletal lapilli in explosive kimberlite eruptions

T. M. Gernon <sup>a,\*</sup>, R. J. Brown <sup>b</sup>, M. A. Tait <sup>c</sup>, T. K. Hincks <sup>d</sup>

<sup>a</sup>*School of Ocean and Earth Science, University of Southampton, Southampton SO14 3ZH, U.K.*

<sup>b</sup>*Department of Earth Sciences, Durham University, Durham DH1 3LE, U.K.*

<sup>c</sup>*Rio Tinto Limited, St George's Terrace, Perth, Western Australia 6000*

<sup>d</sup>*Department of Earth Sciences, University of Bristol, Bristol BS8 1RJ, U.K.*

---

## Abstract

Kimberlites are volatile-rich magmas from mantle depths in excess of 150 km<sup>1,2</sup> and are the primary source of diamonds. Kimberlite volcanism involves the formation of diverging pipes or diatremes<sup>3</sup>, which are the locus of high-intensity explosive eruptions<sup>1,2</sup>. A conspicuous and previously enigmatic feature of diatreme fills are ‘pelletal lapilli’<sup>1,3,4</sup> — well-rounded clasts that consist of an inner ‘seed’ particle with a complex rim, thought to represent quenched juvenile melt<sup>1,5,6</sup>. Such clasts are widely documented in a range of pyroclastic successions on Earth<sup>7,8,9</sup>. New observations of pelletal lapilli show they coincide with a transition from magmatic to pyroclastic behaviour, thus offering fundamental insights into eruption dynamics and constraints on vent conditions. We provide strong evidence that pelletal lapilli form by fluidized spray granulation — a coating process used widely in industrial applications<sup>10,11,12</sup>. We propose that pelletal lapilli are formed when fluid volatile-rich melts intrude into earlier volcanoclastic infill close to the diatreme root zone. Intensive degassing produces a gas jet<sup>13</sup> in which locally-scavenged particles are simultaneously fluidized and coated by a spray of low-viscosity melt. Most fine particles are either agglomerated to pelletal coatings<sup>11,12,14</sup> or ejected by powerful gas flows<sup>1,5</sup>. This type of multi-stage intrusion will result in spatial and temporal variation in the structure and composition of pipe-fill, and consequently will influence local diamond grade and size distributions. A similar origin may apply to pelletal lapilli in other alkaline volcanic rocks including carbonatites, kamafugites and melilitites.

---

\* Corresponding author.

*Email address:* Thomas.Gernon@noc.soton.ac.uk (T. M. Gernon).

## 33 Introduction

34 Kimberlite melts ascend from the Earth’s mantle to the surface in a matter of  
35 hours to days<sup>1,15</sup>. Their diatreme-hosted deposits provide valuable insights into  
36 the dynamics of other volcanic conduits and represent the main source of dia-  
37 monds on Earth. Kimberlite diatremes are subject to a wide range of volcanic  
38 and sedimentary processes and interactions<sup>16,17</sup>, exceptional fossil preserva-  
39 tion<sup>18</sup>, and hydrothermal metamorphism<sup>1,5</sup>. Additionally, the xenoliths and  
40 xenocrysts they contain provide valuable information on the structure and  
41 composition of the deep subcontinental mantle<sup>19,20</sup>.

42 Most volcanoclastic kimberlites contain ubiquitous yet poorly understood com-  
43 posite particles termed ‘pelletal lapilli’<sup>1,2,3,4,6,21</sup>. These are defined as discrete  
44 sub-spherical clasts with a central fragment, mantled by a rim of probable juve-  
45 nile origin<sup>3</sup>. Pelletal lapilli typically range in size from <1 – 60 mm, and occur  
46 both as accessory components of pipe-filling volcanoclastic kimberlites, and as  
47 the main pyroclast type in narrow, steep-sided ‘pipes’ within the diatreme.  
48 These clasts have previously been attributed to incorporation of particles into  
49 liquid spheres in the rising magma<sup>2,8</sup> and rapid unmixing of immiscible liq-  
50 uids<sup>22</sup>. However, these models fail to explain many aspects of their internal  
51 structure, composition and abundance in pyroclastic intrusions. Pelletal lapilli  
52 have been identified globally in a wide range of other alkaline volcanic rocks  
53 including carbonatites<sup>7</sup>, kamafugites<sup>8,23</sup>, melilitites<sup>7,22</sup> and orangeites<sup>9</sup>. They  
54 have also been referred to as ‘tuffisitic lapilli’<sup>7</sup>, ‘spherical lapilli’<sup>24</sup>, ‘spinning  
55 droplets’<sup>8,25</sup> and ‘cored lapilli’<sup>26,27</sup>. Although pelletal lapilli are similar in ap-  
56 pearance and structure to ‘armoured’ (or cored) lapilli<sup>28</sup>, the latter are formed  
57 by accretion of moist fine-grained ash (as opposed to liquid melt) to the cen-  
58 tral fragment<sup>29,30</sup>. Pelletal lapilli share similar properties to particles formed  
59 during industrial fluidized granulation processes, but such processes have not  
60 previously been considered in a geological context.

### 61 *Fluidized spray granulation*

62 Fluidized spray granulation is widely used in industrial engineering to generate  
63 coated granules with specific size, density and physicochemical properties<sup>14</sup>.  
64 The mechanism involves continuous injection of atomizable liquids, solutions  
65 or melts into a powdery fluidized bed<sup>11</sup>, which produces a dispersion of larger  
66 coated granules that are simultaneously dried by the hot fluidizing gas<sup>11,12</sup>.  
67 When gas flows upwards through particles, the point of minimum fluidization  
68 ( $U_{mf}$ ) occurs when the flow velocity ( $U$ ) is sufficiently high to support the  
69 weight of particles without transporting them out of the system<sup>31</sup>.  $U_{mf}$  is  
70 defined according to the semi-empirical Ergun equation<sup>32</sup>:

$$71 \quad \frac{-\Delta P}{h} = 150 \frac{\mu_g \cdot U_g}{x_p^2} \frac{(1 - \epsilon)^2}{\epsilon^3} + 1.75 \frac{\rho_g U_g^2}{x_p} \frac{(1 - \epsilon)}{\epsilon^3} \quad (1)$$

72 where  $\Delta P/h$  is the pressure drop across a bed of height,  $h$ ,  $\rho_g$  is the gas  
 73 density,  $\mu_g$  is the gas dynamic viscosity,  $\epsilon$  is porosity and  $x_p$  is the diameter of  
 74 spherical particles. Fluidized spray granulation is a characteristically steady  
 75 growth process, producing uniform well-rounded particles with a concentric  
 76 layered structure<sup>12</sup>. These physical features are diagnostic of pelletal lapilli in  
 77 kimberlite deposits.

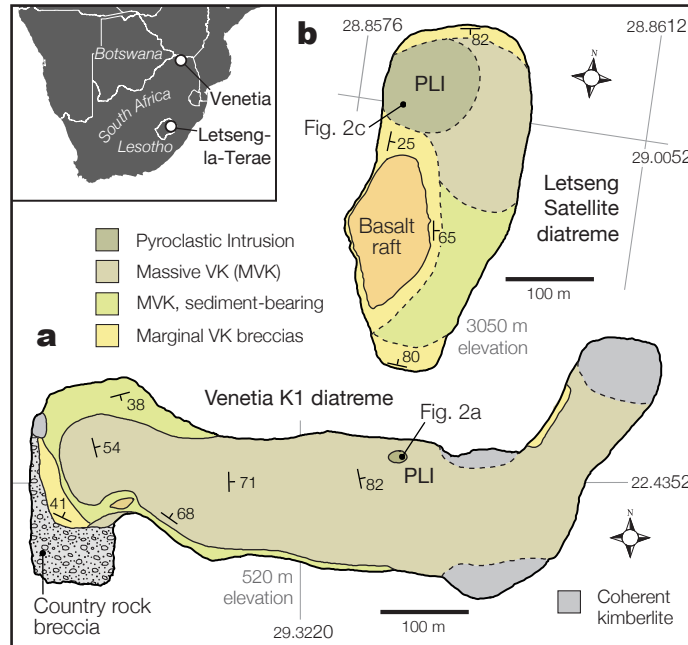


Fig. 1. **Simplified geological maps of the Venetia and Letseng kimberlite pipes.** **a.** Venetia K1 is dominated by massive volcanoclastic kimberlite (MVK, see text for details) with subordinate marginal breccias, sediment-bearing volcanoclastic kimberlite and coherent kimberlite lithofacies. The  $\sim 15$  m wide pelletal-lapilli intrusion (PLI) occurs near the north-central margin of the pipe, where it cross-cuts MVK and is closely associated with numerous minor late-stage dykes. **b.** The Letseng Satellite pipe is also dominated by MVK; pelletal lapilli are confined to a northern circular pipe  $\sim 100$  m wide (modified after ref.<sup>33</sup>). Inset depicts location of the deposits in southern Africa.

## 78 Field observations and results

### 79 *Locality 1: Venetia K1 diatreme, South Africa*

80 Pelletal lapilli occur prominently in two of the world's largest diamond mines,  
 81 Venetia (South Africa) and Letšeng-la-Terae (Lesotho), both well-exposed,  
 82 extensively surveyed<sup>5,6,34</sup> and economically significant localities. The Venetia  
 83 K1 diatreme was emplaced during the late-Cambrian Period (c.  $519 \pm 6$  Ma)<sup>35</sup> into  
 84 metamorphic rocks of the neo-Archaeon—Proterozoic Limpopo  
 85 Mobile Belt (3.3–2.0 Ga). The diatreme (Fig. 1a) is dominated by massive vol-

86 caniclastic kimberlite, MVK (previously termed tuffisitic kimberlite breccia,  
87 TKB, sometimes abbreviated TK)<sup>21</sup>, a characteristically well-mixed lithofa-  
88 cies comprising serpentinized olivine crystals and a polymict range of lithic  
89 clasts<sup>34,36</sup>. The formation of MVK has been attributed to fluidization<sup>1,2,6</sup>, the  
90 scale and context of which is heavily debated<sup>36,37</sup>. Pelletal lapilli (Figs. 2a-b)  
91 are confined to a narrow (10–15 m diameter), discordant and lenticular body  
92 near the northern margin of K1 (Fig. 1a). Although pipe-like, we refer to  
93 these features as pyroclastic intrusions to avoid confusion with the large-scale  
94 (0.5–1 km diameter) pipes or diatremes in which they occur. Field and drill-  
95 core data suggest that the intrusion is a steep-sided tapering cone, associated  
96 with numerous late phlogopite-rich dykes. The intrusion is characteristically  
97 structureless, clast- to matrix-supported and poorly to moderately sorted. It  
98 contains abundant (90 vol.%) coated lapilli-sized, and very rare bomb-sized  
99 clasts (Fig. 2a-b), ranging in diameter from 0.2 – 100 mm (mean,  $\bar{x}$  = 9.4 mm;  
100 Fig. 3a). These pelletal lapilli comprise a sub-angular lithic clast or olivine  
101 macrocryst as their core surrounded by a variably thick coating (generally <1  
102 cm); typically this coating comprises olivine-phlogopite-spinel bearing kimber-  
103 lite with a heavily altered groundmass containing amorphous serpentine and  
104 talc. A concentric alignment of crystals is commonly developed in the coating  
105 around the core (Fig. 2b). In some cases, the pelletal coatings appear to have  
106 partially coalesced.

107 *Locality 2: Letseng-la-Terae Satellite pipe, Lesotho*

108 The Letseng-la-Terae Satellite pipe erupted during the Late Cretaceous Period  
109 (c. 91 Ma<sup>6,33</sup>) through Lower Jurassic flood basalts of the Drakensberg Group.  
110 Pelletal lapilli occur within a steep-sided ( $\sim 80^\circ$ ), 100 m-wide circular intru-  
111 sion. This cross-cuts MVK and marginal inward-dipping volcanoclastic breccias  
112 (Fig. 1b)<sup>33</sup> defining a nested geometry<sup>34</sup>. Pelletal lapilli are characteristically  
113 well rounded (Fig. 2c-d), ranging in size from 60  $\mu\text{m}$  to 61 mm ( $\bar{x}$  = 3.5 mm;  
114 Fig. 3a). Pelletal cores typically constitute mantle<sup>33</sup> and crustal xenoliths, the  
115 most abundant being basaltic lithic clasts (85%) of presumed Drakensberg ori-  
116 gin<sup>6</sup>. The rims to serpentinized olivines (Fig. 2d) typically consist of euhedral  
117 to subhedral olivine phenocrysts, very fine-grained chrome spinel, perovskite  
118 and titanite. The pore space is infilled by a secondary serpentine–diopside  
119 assemblage (Fig. 2e), which further from olivine clusters gives way to calcite<sup>6</sup>.

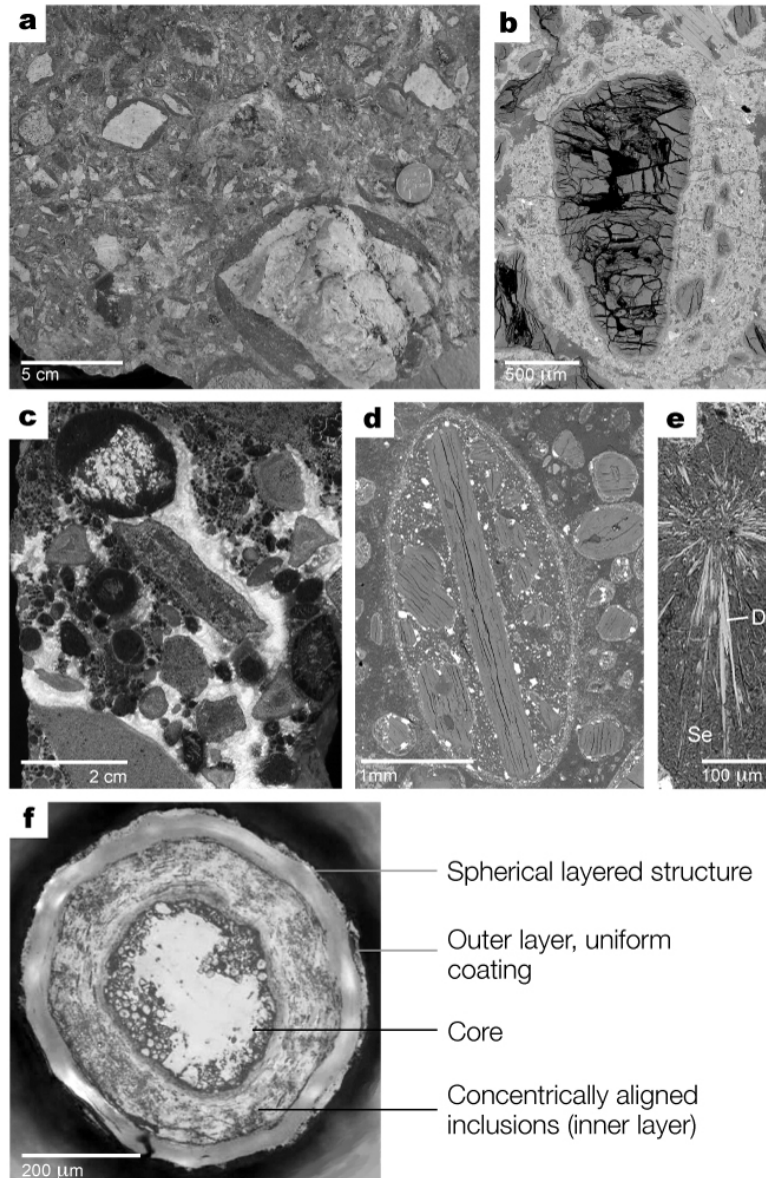


**Fig. 2. Photographs of pelletal lapilli from southern African kimberlites and a synthetic analogue.** **a.** Exposure from the Venetia K1 pyroclastic intrusion showing concentrations of pelletal lapilli, which are characteristically well rounded. **b.** SEM (backscattered-electron) image of a pelletal lapillus from (a), comprising a serpentinised olivine core and fine-grained rim comprising talc, spinel and numerous concentrically aligned micro-phenocrysts. **c.** Hand specimen from Letseng showing circular–elliptical pelletal lapilli and crystals. **d.** SEM image of an elliptical pelletal lapillus from (c); note the incorporation of smaller crystals into the rim. **e.** SEM image of the matrix of (d) showing the inter-growth of void-filling serpentine (Se) and diopside (Di), an assemblage indicative of low-temperature hydrothermal alteration<sup>5</sup>. **f.** For comparison, a synthetic pharmaceutical granule produced by several stages of fluidized granulation; crystalline sugar core surrounded by layers of glucose, talc, polymers and cellulose (after ref.<sup>38</sup>).

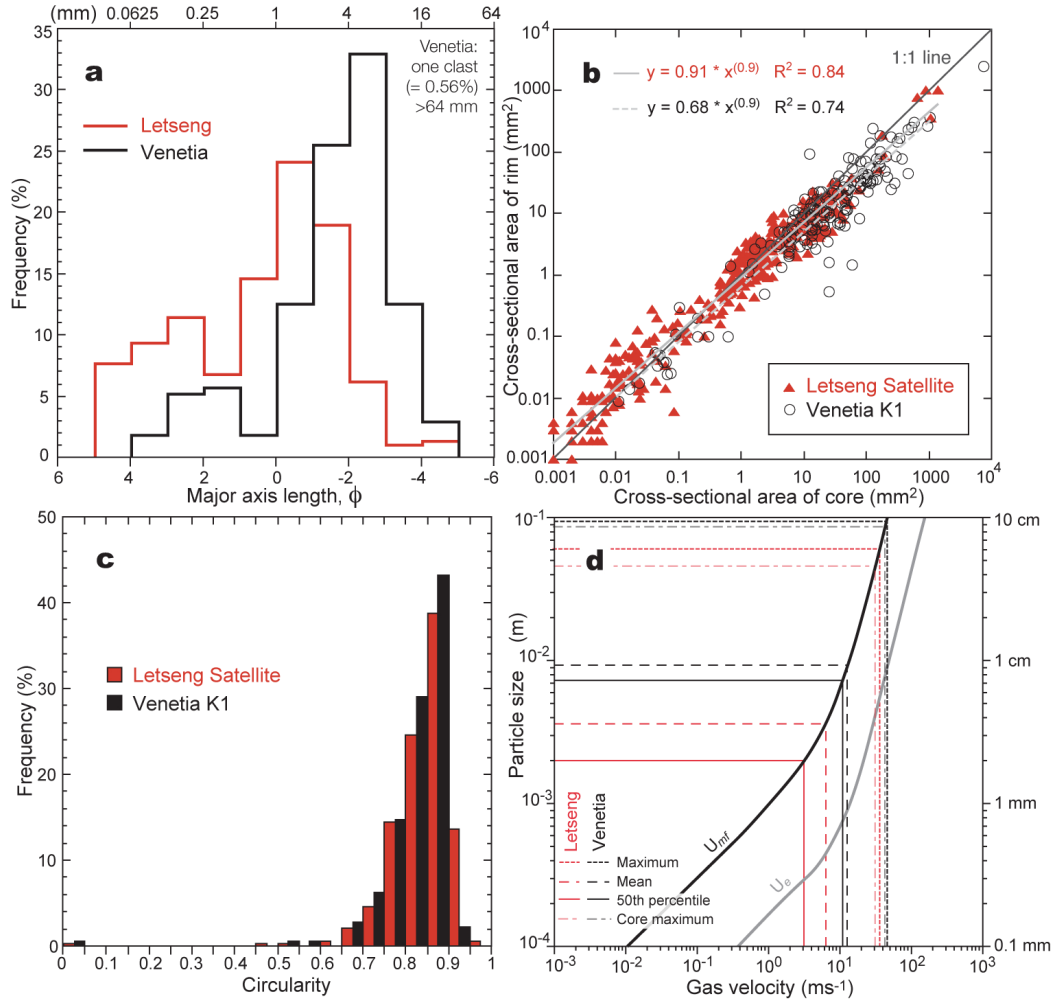


**Fig. 3. Particle size and shape properties of pelletal lapilli from Letseng and Venetia, and the relationship between size and gas velocity.** **a.** Step plot showing the frequency (%) of lapilli versus lapilli size in phi ( $\phi$ ) scale where  $\phi = -\log_2 d$ , and  $d$  is the lapillus long-axis in millimetres. **b.** The area of the rim is plotted against the area of the core for pelletal lapilli from both intrusions. **c.** Histograms showing circularity for pelletal lapilli distributions from Letseng and Venetia (see methods). **d.** Variation in the minimum fluidization velocity ( $U_{mf}$ , equation 1) and escape velocity ( $U_e$ )<sup>39</sup> for crystals and lithic clasts, fluidized by  $\text{CO}_2$  at  $1000^\circ\text{C}$  (modified after ref.<sup>1</sup>). Parameter values are  $\rho_s = 3300 \text{ kg m}^{-3}$ , to represent olivine crystals and dense lithic clasts; voidage,  $\epsilon_{mf} = 0.5$  and viscosity,  $\mu = 4.62 \times 10^{-6} \text{ Pa s}$ . The graph shows the gas velocities required to reach  $U_{mf}$  and  $U_e$  for a range of characteristic particle sizes (shown) for Letseng and Venetia. Note that  $U_{mf}$  of the maximum lapilli size  $\simeq U_e$  of the mean lapilli size. The window between  $U_{mf}$  and  $U_e$  shows that a range of particle sizes can be supported (i.e. fluidized) but not ejected.

121 *Characteristics of pelletal lapilli*

122 The characteristics of observed pelletal lapilli (Figs. 2-3) are indicative of flu-  
 123 idized spray granulation<sup>11,12</sup>. This process generates well-rounded composite  
 124 particles<sup>12</sup>, uniformly coated<sup>40</sup> with layered concentrically-aligned inclusions  
 125 (Fig. 2f)<sup>38</sup>. For both deposits, data show a moderate to strong positive cor-  
 126 relation between the cross-sectional area of the seed particle and that of the  
 127 coating (Fig. 3b), suggesting a uniform coating process and underlying scale  
 128 invariance. Particle growth rate generally increases with increasing particle  
 129 diameter<sup>11</sup>, due to their greater surface area. However, in this instance larger  
 130 clasts have proportionally less rim material (gradient  $< 1$ ; Fig. 3b). Larger  
 131 clasts have higher inertia, requiring higher sustained velocities for fluidiza-  
 132 tion, and experiencing increased abrasion at lower velocities ( $U < U_{mf}$ ). The  
 133 circular-elliptical geometry exhibited by pelletal lapilli (Figs. 2 & 3c) suggests  
 134 their formation is governed by surface tension<sup>1</sup>, a major variable in fluidized  
 135 spray granulation<sup>40</sup>. The presence of multiple rims and concentrically aligned  
 136 phenocrysts in some pelletal lapilli (Fig. 2b)<sup>22</sup> is suggestive of a systematic  
 137 multi-stage layering process<sup>12</sup>.

138 Another key characteristic of spray granulation is the generation of a narrow  
 139 particle size distribution<sup>14</sup>, partly due to the agglomeration of fines<sup>11,14</sup>. This  
 140 is evidenced by the incorporation of small discrete rimmed crystals within  
 141 larger pelletal rims (Fig. 2b & d). Although the Venetia and Letseng size  
 142 distributions are not strictly narrow (Fig. 3a), the host and proposed source  
 143 material (i.e. MVK, see Fig. 1) has a remarkably wide size distribution with  
 144 observed crystal and lithic inclusions ranging from 0.015–~800 mm (6 to -  
 145  $9.7\phi$ )<sup>34,36</sup>. Venetia MVK contains a high proportion of small olivine crystals  
 146 (mode  $\simeq 0.2$  mm) with proportionally fewer larger lithic clasts (mode  $\simeq 23$   
 147 mm) resulting in a bimodal joint size distribution (Fig. 6 in ref.<sup>34</sup>). Lapilli  
 148 sizes at Letseng and Venetia also show slight bimodality (Fig. 3a), but the  
 149 size range is more restricted (0.03–32 mm; 5 to  $-5\phi$ ) with a higher proportion  
 150 of larger lapilli (Venetia mode = 5.7 mm) and a relative paucity of fine-grained  
 151 particles ( $< 0.5$  mm; Fig. 3a).

152 *Constraints on gas velocity*

153 To fluidize and coat the largest observed pelletal lapilli in the intrusions, gas  
 154 velocities must have reached  $\sim 45$  m/s (Fig. 3d), broadly consistent with other  
 155 estimates for MVK<sup>1,34,36</sup>. We emphasize, however, that the local velocity due  
 156 to gas bubbles and jets is normally several times greater than the characteristic  
 157 velocity of the bed<sup>13,31</sup>. Additionally, the tapered geometry gives rise to a  
 158 circulating fluidized system<sup>31</sup> enabling a wide range of pelletal lapilli sizes  
 159 to coexist in equilibrium. For Venetia,  $U_{mf}$  of the maximum-size lapilli is  
 160 approximately equal to the escape velocity  $U_e$  (the velocity at which particles

161 escape from the system)<sup>39</sup> of the median-size lapilli (Fig. 3d). This implies  
162 there must be significant local variation in gas velocity to sustain fluidization  
163 across the range of particle sizes observed whilst retaining the smaller size  
164 fraction. For Letseng, median particle size is considerably lower ( $\sim 2$  mm,  $U_{mf}$   
165 = 3 m/s) suggesting greater variation in gas velocity, which can be explained  
166 by the wider vent diameter and more pronounced tapering. Clasts too large  
167 to become fluidized will behave as dispersed objects<sup>36</sup>.

168 Given the high volatile contents required to generate melts of kimberlite com-  
169 position (5–10 wt.%)<sup>41,42</sup>, we argue that gas flow-rates required to fluidize  
170 clasts are easily achievable during degassing of a kimberlite magma. Assum-  
171 ing a pyroclastic intrusion diameter of 10 m, and taking gas velocities of 12  
172  $\text{ms}^{-1}$  (for the mean of the Venetia distribution; see Fig. 3d) and 45  $\text{ms}^{-1}$  (for  
173 the maximum size; see Fig. 3d), we would require gas flow-rates on the order of  
174  $942 \text{ m}^3\text{s}^{-1}$  to  $3.5 \times 10^3 \text{ m}^3\text{s}^{-1}$  respectively. Our previous calculations<sup>36</sup> show  
175 that degassing in kimberlite root zones could result in gas mass flow-rates as  
176 high as  $3 \times 10^6 \text{ m}^3\text{s}^{-1}$ , so the above estimates seem conservative. Given these  
177 estimates, a hypothetical kimberlite dyke segment of conservative length,  $h =$   
178 10 km, breadth,  $b = 50$  m and width,  $2w = 2$  m, containing 10% volatiles,  
179 could release sufficient gas volumes to fluidize the entire intrusion-fill for tens  
180 of seconds to several minutes. As such, a degassing dyke could sustain a gas  
181 jet for long enough to efficiently entrain a significant amount of recycled pyro-  
182 clasts. These results are not surprising, as comparable basaltic systems (e.g.,  
183 persistently active volcanoes) can release large volumes of gas with broadly  
184 equivalent mass fluxes over significant periods of time<sup>43</sup>, without necessarily  
185 erupting any significant volume of degassed lava<sup>44</sup>.

### 186 *Formation of pelletal lapilli*

187 We propose that fluidized spray granulation occurs when a new pulse of kim-  
188 berlite magma intrudes into unconsolidated pyroclastic deposits within the  
189 diatrema (Fig. 4a). The magma is transported through a dyke or system of  
190 dykes in the deep feeding system, which at low to intermediate levels drive  
191 explosive volcanic flows<sup>45</sup> within the tapered pyroclastic intrusion. At the in-  
192 terface between the dyke and conduit, intensive volatile exsolution results in  
193 the formation of a gas jet<sup>13</sup> where velocities are sufficiently high (order of  
194 tens of metres per second)<sup>1,36</sup> to fluidize the majority of particles (Fig. 3d)  
195 and inhibit formation of liquid bridges between clasts<sup>12</sup>. Particles from MVK  
196 are entrained into the jet due to the drag force exerted by the fluidizing gas  
197 (Fig. 4a)<sup>11</sup>. Degassing is accompanied by a continuous spray of low-viscosity  
198 melt into the gas jet region<sup>11</sup>. Melt droplets are provided by fragmentation  
199 – the catastrophic bursting of bubbles to form a gassy spray<sup>46</sup>. The frag-  
200 mentation level (Fig. 4a) will vary depending on the tensile strength of the  
201 magma<sup>46</sup>, which will be influenced by the ambient pressure-temperature con-  
202 ditions, magma rheology<sup>47</sup> and magma water content<sup>1,46</sup>. As melt droplets are  
203 deposited on the hot particles, they produce a thin film governed by surface



204 tension, which dries rapidly to form a solid uniform coating<sup>11</sup> (Fig. 4a-b).  
 205 Most of the very fine ash (<500  $\mu\text{m}$ ) is either agglomerated to the pelletal  
 206 coatings<sup>11,12,14</sup> or elutriated by powerful gas flows<sup>1,5</sup>. Due to a combination  
 207 of cohesion, high gas velocities and high fluid pressures, a fracture develops  
 208 and the fluidized dispersion ascends turbulently through the diatreme fill with  
 209 limited attrition and breakage (Fig. 4b). Fluidization may be promoted by a  
 210 sudden drop in pressure and corresponding increase in gas exsolution accom-  
 211 panying fracture development<sup>48</sup>. The lack of segregation of large lithic clasts  
 212 indicates a relatively rapid termination of gas supply<sup>36</sup>.

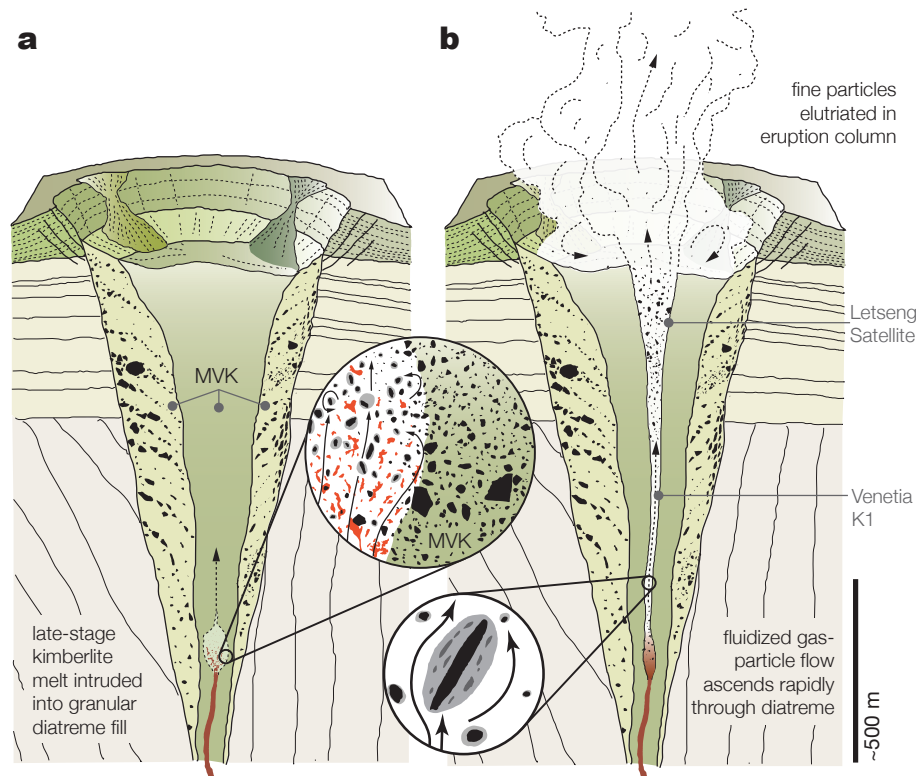


Fig. 4. **Schematic showing the formation of pelletal lapilli in kimberlite diatremes** (see text for details). **a.** A fluid, volatile-rich melt is intruded into loose diatreme fill; intensive volatile exsolution produces a gas-jet, opening up a fracture within MVK deposits; inset: particles from MVK are entrained and fluidized in the gas jet and uniformly coated by a spray of melt (red); fine particles are either agglomerated to pelletal coatings or elutriated by strong gas flows. **b.** Driven by gas expansion and exsolution in the jet region, gas-particle dispersion ascends rapidly (>20 m/s) and turbulently through the diatreme and the eruption is abruptly ended.

213 Our observations from Venetia and Letseng can be explained by dyke intru-  
 214 sion resulting in explosive flow processes within a narrow conduit. However,  
 215 we recognise that this model will not explain all occurrences of pelletal lapilli  
 216 globally, and that other important granule-forming processes may operate dur-  
 217 ing eruptions. An example might include Hawaiian-style lava fountains at the  
 218 surface, where it is common for melt and gas phases to coincide with crystals

219 and entrained clasts<sup>49</sup>. It is not difficult to conceive situations in which such  
220 particles could be fully supported by the viscous drag of escaping volatiles,  
221 and simultaneously coated by a spray of fragmented low-viscosity melt. This  
222 process would provide an opportunity for recycling of previously generated  
223 pyroclasts. However, our model (see Fig. 4) provides a mechanism for pelletal  
224 lapilli to form at depth in pyroclastic intrusions within the vent, consistent  
225 with field relationships observed at Venetia and Letseng. In this model, pel-  
226 letal lapilli are also expected to get erupted explosively and ejected during  
227 degassing (see Fig. 4b), producing deposits at the surface in which pelletal  
228 lapilli are volumetrically substantial.

### 229 *Occurrence of pelletal lapilli in MVK*

230 Several mechanisms could lead to incorporation of pelletal lapilli into more  
231 typical vent-filling MVK, as observed in other pipes such as Letseng (main  
232 pipe), Wesselton, Lemphane, Lihobong, Kao and Premier<sup>3,50</sup>. For example,  
233 pelletal lapilli ejected at the surface will get deposited in marginal bedded  
234 regions, which are capable of subsiding to deep levels in the pipe during sub-  
235 sequent explosive bursts at depth<sup>51,52,53,54</sup>, and gas-fluidization of the pipe-  
236 fill<sup>36,55</sup>. Such large-scale fluidization processes are thought to promote thor-  
237 ough mixing of pre-existing pyroclastic material<sup>34,36</sup> (including pelletal lapilli),  
238 as the vigorously fluidized dispersion effectively erodes and entrains loose ma-  
239 terial from the marginal subsided strata in the pipe<sup>55</sup>. It is very likely that  
240 successive eruptive phases would disrupt and disaggregate pre-existing pyro-  
241 clastic intrusions, and thereby mix assemblages of pelletal lapilli together with  
242 several phases of MVK. This model is supported by the presence of steep in-  
243 ternal contacts in kimberlite pipe-fills, separating distinct eruptive units with  
244 variable particle size distributions<sup>34,36</sup>.

245 Fluidized spray granulation may also help explain the welding of pyroclasts  
246 from low-viscosity magmas<sup>56</sup>, and complex ‘transition zones’ between hy-  
247 pabyssal and diatrema-facies kimberlites<sup>21,57,58</sup>. Within the Venetia K1 in-  
248 trusion, occasional coalesced lapilli boundaries suggest that clasts either ag-  
249 glomerated during circulation or may have remained hot and partially molten  
250 during emplacement. Although sprayed kimberlite melt is likely to solidify  
251 rapidly upon contact with lithic lapilli, high magma supply rates may lead  
252 to sustained high temperatures and the system becoming dominantly viscous  
253 with particle sintering and agglutination<sup>59</sup>. This would explain observed gra-  
254 dations to non-welded deposits and overlaps in texture and composition with  
255 adjacent pyroclastic deposits<sup>56</sup>.

256 **Concluding remarks**

257 The origin of pelletal lapilli is important for understanding how magmatic py-  
258 roclasts are transported to the surface during explosive eruptions. Observed  
259 differences in juvenile composition may signify a magma with a different man-  
260 tle provenance, or one that had differentiated at depth prior to ascent<sup>60</sup>. Any  
261 resulting compositional differences may be significant in terms of diamond  
262 grade (carats per tonne), size and quality. Recognising the structurally variable  
263 nature of the pipe-fill is also important for economic forecasting. For example,  
264 the Letseng pelletal lapilli intrusion has yielded a relatively high number of  
265 large diamonds (106–215 cts), compared to the surrounding pipe-fill<sup>33</sup>.

266 Spray granulation requires a strong fluidizing gas flow, so our model sheds  
267 new light on the role and magnitude of fluidization in kimberlite volcanic  
268 systems<sup>37</sup>. Our constraints on gas velocity provide important new inputs into  
269 thermodynamic models of kimberlite ascent and eruption, estimates of gas  
270 budget, and possibly even magma rheology. The ability to tightly constrain  
271 gas velocities is significant, as it enables estimation of the maximum diamond  
272 size transported in the flow. Gas-fluidization and magma coating processes are  
273 also likely to affect diamond surface properties.

274 Our observations also have important implications for understanding pyro-  
275 clastic processes in conduits of active volcanoes (e.g. Ol Doinyo Lengai) where  
276 episodes of ash venting (commonly attributed to fluidization) have been re-  
277 lated to changes in eruptive activity. In such settings, pressurised CO<sub>2</sub> will  
278 flow through volcanoclastic deposits in the vent and crater on its way to the  
279 surface, and is likely to fluidize some of the granular material whilst ejecting  
280 the finer particles. The gas source is different but gives rise to the same phe-  
281 nomena. Our results add support to the hypothesis that pelletal lapilli in other  
282 volcanic settings are formed within the diatreme as opposed to the eruption  
283 column<sup>27</sup>.

284 Most diatremes worldwide contain minor hypabyssal intrusions that cross-cut  
285 pyroclastic lithofacies<sup>1,3</sup>. When such melts penetrate loose granular deposits  
286 in the presence of rapid gas flows, we envisage that some degree of spray gran-  
287 ulation is inevitable. Based on the abundance of pelletal lapilli in volcanic de-  
288 posits worldwide<sup>1,3,4,7,8,22</sup>, fluidized spray granulation is likely a fundamental,  
289 but hitherto unrecognized physical process during volcanic conduit formation.

## 290 **Methods**

291 Hand specimens containing pelletal lapilli were collected from both pyroclastic in-  
292 trusions (Fig. 1) and analysed petrographically using optical and scanning electron  
293 microscopy (HITACHI S-3500N). High-resolution digital photographs (scaled and  
294 oriented) were taken of polished slabs and bench exposures. Particle size distribution  
295 analysis was carried out following the technique outlined in ref.<sup>34</sup>. Because there is  
296 naturally a size limit to observable particles at any scale, samples were analysed at  
297 several overlapping scales<sup>34</sup>. Individual pelletal lapilli, lithic fragments and serpen-  
298 tinized olivine crystals were manually identified and digitized in the Adobe Illustr-  
299 ator (CS4) graphics package, and the resulting bitmap images were then processed  
300 in the image analysis software package, ImageJ (developed by the U.S. National  
301 Institute of Health; <http://rsb.info.nih.gov/ij/download.html>) following ref.<sup>6</sup>. This  
302 provided major and minor axis measurements, cross-sectional areas for cores and  
303 rims, and circularity values (defined as  $4\pi \times \text{area}/\text{perimeter}^2$ ; i.e. 1.0 indicates a  
304 perfect circle).

## 305 **Acknowledgements**

306 This research was supported by De Beers Group Services UK, who facilitated access  
307 to Venetia Mine for fieldwork. We also acknowledge Letšeng Diamonds (Pty) Ltd, in  
308 particular K. Whitelock and C. Palmer for onsite discussions and allowing access to  
309 the Letšeng Diamond Mine. We are grateful to S. Sparks, M. Gilbertson and M. Field  
310 for discussions, and thank E. Rohling, P. Wilson and R. Howlett for comments on  
311 an earlier version of this paper. Fig. 2f (modified after ref.<sup>38</sup>) is reproduced with the  
312 permission of Oxford University Press. We thank James Head III and Kelly Russell  
313 for their constructive reviews that helped to greatly improve the manuscript.

## 314 **Author contributions**

315 T.G. directed the research; T.G., R.B. and M.T. carried out the fieldwork and  
316 sampling; T.G. and R.B. performed petrographic analysis and analyzed particle  
317 size distributions; T.G. and T.H. wrote the paper, T.G. drafted the figures and T.H.  
318 assisted with plotting the maps. All authors discussed the results and contributed  
319 to the final manuscript.

## 320 **References**

- 321 1. Sparks, R. S. J., Baker, L., Brown, R., Field, M., Schumacher, J., Stripp, G.,  
322 and Walters, A. Dynamical constraints on kimberlite volcanism. *Journal of*

- 323 *Volcanology and Geothermal Research* **155**, 18–48 (2006).
- 324 2. Wilson, L. and Head, J. W. An integrated model of kimberlite ascent and  
325 eruption. *Nature* **447**, 53–57 (2007).
- 326 3. Mitchell, R. H. *Kimberlites: Mineralogy, Geochemistry, and Petrology*. Plenum  
327 Press, (1986).
- 328 4. Clement, C. R. and Skinner, E. M. W. A textural-genetic classification of  
329 kimberlites. *South African Journal of Geology* **88**(2), 403–409 (1985).
- 330 5. Stripp, G. R., Field, M., Schumacher, J. C., Sparks, R. S. J., and Cressey, G.  
331 Post emplacement serpentinization and related hydrothermal metamorphism in  
332 a kimberlite from Venetia, South Africa. *Journal of Metamorphic Geology* **24**,  
333 515–534 (2006).
- 334 6. Gernon, T. M., Sparks, R. S. J., and Field, M. Degassing structures in volcani-  
335 clastic kimberlite: examples from southern African kimberlite pipes. *Journal of*  
336 *Volcanology and Geothermal Research* **174**(1-3), 186–194 (2008).
- 337 7. Stoppa, F. The San Venanzo maar and tuff ring, Umbria, Italy: eruptive be-  
338 haviour of a carbonatite-melilitite volcano. *Bulletin of Volcanology* **57**(7), 563–  
339 577 (1996).
- 340 8. Junqueira-Brod, T. C., Brod, J. A., Thompson, R. N., and Gibson, S. A. Spin-  
341 ning droplets: a conspicuous lapilli-size structure in kamafugitic diatremes of  
342 southern Goiás, Brazil. *Revisita Brasileira de Geociencias* **29**(3), 437–440  
343 (1999).
- 344 9. Mitchell, R. H. *Kimberlites, orangeites, and related rocks*. Plenum Press, (1995).
- 345 10. Lister, J. D., Hapgood, K. P., Michaels, J. N., Sims, A., Roberts, M., Kameneni,  
346 S. K., and Hsu, T. Liquid distribution in wet granulation: dimensionless spray  
347 flux. *Powder Technology* **114**, 32–39 (2001).
- 348 11. Zank, J., Kind, M., and Schlünder, E. U. Particle growth and droplet deposition  
349 in fluidised bed granulation. *Powder Technology* **120**, 76–81 (2001).
- 350 12. Christoph-Link, K. and Schlünder, E. U. Fluidized bed spray granulation: In-  
351 vestigation of the coating process on a single sphere. *Chemical Engineering and*  
352 *Processing* **36**, 443–457 (1997).
- 353 13. Roach, P. E. The penetration of jets into fluidized beds. *Fluid Dynamics*  
354 *Research* **11**, 197–216 (1993).
- 355 14. Rajniak, P., Mancinelli, C., Chern, R. T., Stepanek, F., Farber, L., and Hill,  
356 B. T. Experimental study of wet granulation in fluidized bed: Impact of the  
357 binder properties on the granule morphology. *International Journal of Phar-*  
358 *maceutics* **334**, 92–102 (2007).
- 359 15. Canil, D. and Fedortchouk, Y. Garnet dissolution and the emplacement of  
360 kimberlites. *Earth and Planetary Science Letters* **167**(3-4), 227–237 (1999).
- 361 16. Smith, R. M. H. Sedimentation and palaeoenvironments of Late Cretaceous  
362 crater-lake deposits in Bushmanland, South Africa. *Sedimentology* **33**, 369–386  
363 (1986).
- 364 17. Gernon, T. M., Field, M., and Sparks, R. S. J. Depositional processes in a  
365 kimberlite crater: the Upper Cretaceous Orapa South Pipe (Botswana). *Sedi-*  
366 *mentology* **56**(3), 623–643 (2009).
- 367 18. Rayner, R. J., Bamford, K., Brothers, D. I., Dippenaar-Schoeman, X., and  
368 McKay, I. J. Cretaceous fossils from the Orapa diamond mine. *Palaeontologia*  
369 *Africana* **33**, 55–65 (1998).

- 370 19. Walker, R. J., Carlson, R. W., Shirley, S. B., and Boyd, F. R. Os, Sr, Nd, and  
371 Pb isotope systematics of southern African peridotite xenoliths: Implications for  
372 the chemical evolution of subcontinental mantle. *Geochimica et Cosmochimica*  
373 *Acta* **53**(7), 1583–1595 (1989).
- 374 20. Torsvik, T. H., Burke, K., Steinberger, B., Webb, S. J., and Ashwal, D. Dia-  
375 monds sampled by plumes from the core-mantle boundary. *Nature* **466**, 352–355  
376 (2010).
- 377 21. Hetman, C. M., Smith, B. H. S., Paul, J. L., and Winter, F. Geology of the Gah-  
378 cho Kué kimberlite pipes, NWT, Canada: root to diatreme magmatic transition  
379 zones. *Lithos* **76**(1-4), 51–74 (2004).
- 380 22. Lloyd, F. E. and Stoppa, F. Pelletal lapilli in diatremes - Some inspiration from  
381 the old masters. *Geolines* **15**, 65–71 (2003).
- 382 23. Stoppa, F., Woolley, A. R., and Cundari, A. Extension of the melilite-  
383 carbonatite province in the Apennines of Italy: the kamafugite of Grotta del  
384 Cervo, Abruzzo. *Mineralogical Magazine* **66**(4), 555–574 (2002).
- 385 24. Keller, J. Carbonatitic volcanism in the Kaiserstuhl alkaline complex: evidence  
386 for highly fluid carbonatitic melts at the Earth’s surface. *Journal of Volcanology*  
387 *and Geothermal Research* **9**, 423–431 (1981).
- 388 25. Junqueira-Brod, T. C., Gaspar, J. C., Brod, J. A., and Kafino, C. V. Ka-  
389 mafugitic diatremes: their textures and field relationships with examples from  
390 the Goiás Alkaline Province, Brazil. *Journal of South American Earth Sciences*  
391 **18**(3-4), 337–353 (2005).
- 392 26. Lefebvre, N., Kopylova, M., and Kivi, K. Archean calc-alkaline lamprophyres of  
393 Wawa, Ontario, Canada: Unconventional diamondiferous volcanoclastic rocks.  
394 *Precambrian Research* **138**(1-2), 57–87 (2005).
- 395 27. Stoppa, F., Lloyd, F. E., Tranquilli, A., and Schiazza, M. Comment on: De-  
396 velopment of spheroid “composite” bombs by welding of juvenile spinning and  
397 isotropic droplets inside a mafic “eruption” column by Carracedo Sánchez et  
398 al. (2009). *Journal of Volcanology and Geothermal Research* **204**(1-4), 107–116  
399 (2011).
- 400 28. Kurszlaukis, S. and Barnett, W. P. Volcanological and structural aspects of  
401 the Venetia kimberlite cluster - a case study of South African kimberlite maar-  
402 diatreme volcanoes. *South African Journal of Geology* **106**, 165–192 (2003).
- 403 29. McPhie, J., Doyle, M., and Allen, R. *Volcanic textures: A guide to the inter-*  
404 *pretation of textures in volcanic rocks*. Tasmanian Government Printing Office,  
405 Tasmania, (1993).
- 406 30. Junqueira-Brod, T. C., Brod, J. A., Gaspar, J. C., and Jost, H. Kamafugitic  
407 diatremes: facies characterisation and genesis-examples from the Goiás Alkaline  
408 Province, Brazil. *Lithos* **76**(1-4), 261–282 (2004).
- 409 31. Davidson, J. F. and Harrison, D. *Fluidised Particles*. Cambridge University  
410 Press, (1963).
- 411 32. Ergun, S. Fluid flow through packed columns. *Chemical Engineering Progress*  
412 **48**(2), 89–94 (1952).
- 413 33. Palmer, C. E., Ward, J. D., Stiefenhofer, J., and Whitelock, T. K. Volcanolog-  
414 ical processes and their effect on diamond distribution in the Letšeng Satellite  
415 Pipe, Lesotho. In *9th International Kimberlite Conference, Extended Abstracts*,  
416 number 9IKC-A-00096, (2008).

- 417 34. Walters, A. L., Phillips, J. C., Brown, R. J., Field, M., Gernon, T., Stripp, G.,  
418 and Sparks, R. S. J. The role of fluidisation in the formation of volcanoclastic  
419 kimberlite: grain size observations and experimental investigation. *Journal of*  
420 *Volcanology and Geothermal Research* **155**, 119–137 (2006).
- 421 35. Phillips, D., Kiviets, G. B., Barton, E. S., Smith, C. B., Viljoen, K. S., and  
422 Fourie, L. F.  $^{40}\text{Ar}/^{39}\text{Ar}$  dating of kimberlites and related rocks: problems and  
423 solutions. In Proceedings of the 7<sup>th</sup> International Kimberlite Conference, Cape  
424 Town, Gurney, J. J., Gurney, J. L., Pascoe, M. D., and Richardson, S. J., editors,  
425 677–687, (1999).
- 426 36. Gernon, T. M., Gilbertson, M. A., Sparks, R. S. J., and Field, M. The role  
427 of gas-fluidisation in the formation of massive volcanoclastic kimberlite. *Lithos*  
428 **112S**, 439–451 (2009).
- 429 37. Brown, R. J., Field, M., Gernon, T. M., Gilbertson, M. A., and Sparks, R.  
430 S. J. Problems with an in-vent column collapse model for the emplacement  
431 of massive volcanoclastic kimberlite. *Journal of Volcanology and Geothermal*  
432 *Research* **178**(4), 847–850 (2008).
- 433 38. Jacob, L. J., Neuberger, L., and Lawrence-Collins, L. J. Pharmaceutical Hold-  
434 ings Ltd v Ratiopharm GmbH; Napp Pharmaceutical Holdings Ltd v Sandoz  
435 Ltd. *RPC* **126**(8), 539–569 (2009).
- 436 39. Sparks, R. S. J. Grain-size variations in ignimbrites and implications for the  
437 transport of pyroclastic flows. *Sedimentology* **23**, 147–188 (1976).
- 438 40. Panda, R. C., Zank, J., and Martin, H. Experimental investigation of droplet  
439 deposition on a single particle. *Chemical Engineering Journal* **83**, 1–5 (2001).
- 440 41. Fedortchouk, Y. and Canil, D. Intensive variables in kimberlite magmas, Lac  
441 de Gras, Canada and implications for diamond survival. *Journal of Petrology*  
442 **45**(9), 1725–1745 (2004).
- 443 42. Sparks, R. S. J., Brooker, R. A., Field, M., Kavanagh, J., Schumacher, J. C.,  
444 Walter, M. J., and White, J. The nature of erupting kimberlite melts. *Lithos*  
445 **112**(1), 429–438 (2009).
- 446 43. Allard, P., Carbonnelle, J., Métrich, N., Loyer, H., and Zettwoog, P. Sulphur  
447 output and magma degassing budget of Stromboli volcano. *Nature* **368**, 326–330  
448 (1994).
- 449 44. Menand, T. and Phillips, J. C. Gas segregation in dykes and sills. *Journal of*  
450 *Volcanology and Geothermal Research* **159**(4), 393–408 (2007).
- 451 45. Costa, A., Sparks, R. S. J., Macedonio, G., and Melnik, O. Effects of wall-  
452 rock elasticity on magma flow in dykes during explosive eruptions. *Earth and*  
453 *Planetary Science Letters* **288**, 455–462 (2009).
- 454 46. Zhang, Y. A criterion for the fragmentation of bubbly magma based on brittle  
455 failure theory. *Nature* **402**, 648–650 (1999).
- 456 47. Alidibirov, M. and Dingwell, D. B. Magma fragmentation by rapid decompres-  
457 sion. *Nature* **380**, 146–148 (1996).
- 458 48. Kokelaar, B. P. Fluidization of wet sediments during the emplacement and  
459 cooling of various igneous bodies. *Journal of the Geological Society, London*  
460 **139**(1), 21–33 (1982).
- 461 49. Parfitt, E. A. and Wilson, L. A Plinian treatment of fallout from Hawaiian  
462 lava fountains. *Journal of Volcanology and Geothermal Research* **88**(1-2), 67–  
463 75 (1999).

- 464 50. Mitchell, R. H., Skinner, E. M. W., and Smith, B. H. S. Tuffisitic kimberlites  
465 from the Wesselton Mine, South Africa: Mineralogical characteristics relevant  
466 to their formation. *Lithos* **112S**, 452–464 (2009).
- 467 51. Hearn, B. C. Diatremes with kimberlitic affinities in north-central Montana.  
468 *Science* **159**, 622–625 (1968).
- 469 52. Hawthorne, J. B. Model of a kimberlite pipe. *Physics and Chemistry of the*  
470 *Earth* **9**, 1–15 (1975).
- 471 53. Lorenz, V. Formation of phreatomagmatic maar-diatreme volcanoes and its  
472 relevance to kimberlite diatremes. *Physics and Chemistry of the Earth* **9**, 17–29  
473 (1975).
- 474 54. Lorenz, V. On the growth of maars and diatremes and its relevance to the  
475 formation of tuff rings. *Bulletin of Volcanology* **48**, 265–274 (1986).
- 476 55. Gernon, T. M., Gilbertson, M. A., Sparks, R. S. J., and Field, M. Gas-  
477 fluidisation in an experimental tapered bed: insights into processes in diverging  
478 volcanic conduits. *Journal of Volcanology and Geothermal Research* **174**(1-3),  
479 49–56 (2008).
- 480 56. Brown, R. J., Buse, B., Sparks, R. S. J., and Field, M. On the welding of  
481 pyroclasts from very low-viscosity magmas: examples from kimberlite volcanoes.  
482 *The Journal of Geology* **116**(4), 354–374 (2008).
- 483 57. Skinner, E. M. W. and Marsh, J. S. Distinct kimberlite pipe classes with con-  
484 trasting eruption processes. *Lithos* **76**, 183–200 (2004).
- 485 58. Seghedi, I., Maicher, D., and Kurszlaukis, S. Volcanology of Tuzo pipe (Gahcho  
486 Kué cluster) - root-diatreme processes re-interpreted. *Lithos* **112S**, 553–565  
487 (2009).
- 488 59. Jozwiakowki, M. J., Jones, D. M., and Franz, R. M. Characterization of a hot-  
489 melt fluid bed coating process for fine granules. *Pharmaceutical Research* **7**(11),  
490 1119–1126 (1990).
- 491 60. Mitchell, R. H. Petrology of hypabyssal kimberlites: Relevance to primary  
492 magma compositions. *Journal of Volcanology and Geothermal Research* **174**(1-  
493 3), 1–8 (2008).